

Article

Implementation of Optimal Scheduling Algorithm for Multi-Functional Battery Energy Storage System

Hee-Jun Cha ¹ , Sung-Eun Lee ² and Dongjun Won ^{1,*}¹ Department of Electrical Engineering, Inha University, 100, Inha-ro, Nam-gu, Incheon 402-751, Korea; chj119119@gmail.com² Korea Electric Power Research Institute (KEPRI), Korea Electric Power Company (KEPCO), 105 Munji-Ro, Yuseong-gu, Daejeon 34056, Korea; sungeun.lee@kepc.co.kr

* Correspondence: djwon@inha.ac.kr; Tel.: +82-32-860-7404

Received: 1 February 2019; Accepted: 2 April 2019; Published: 8 April 2019



Abstract: Energy storage system (ESS) can play a positive role in the power system due to its ability to store, charge and discharge energy. Additionally, it can be installed in various capacities, so it can be used in the transmission and distribution system and even at home. In this paper, the proposed algorithm for economic optimal scheduling of ESS linked to transmission systems in the Korean electricity market is proposed and incorporated into the BESS (battery energy storage system) demonstration test center. The proposed algorithm considers the energy arbitrage operation through SMP (system marginal price) and operation considering the REC (renewable energy certification) weight of the connected wind farm and frequency regulation service. In addition, the proposed algorithm was developed so that the SOC (state-of-charge) of the ESS could be separated into two virtual SOCs to participate in different markets and generate revenue. The proposed algorithm was simulated and verified through Matlab and loaded into the demonstration system using the Matlab “Runtime” function.

Keywords: energy storage system (ESS); renewable energy certification (REC); arbitrage; frequency regulation; mixed integer linear programming; optimization scheduling; Matlab runtime

1. Introduction

ESS (energy storage system) is capable of storing electric energy, and is capable of charging and discharging, so that it can be used in many aspects of power systems, such as system operators or consumers. In addition, as the ESS technology develops, the installation price is lowered, so that a plurality of batteries can be installed and utilized in the transmission system. ESS can take advantage of various functions depending on installation location and capacity. In the transmission system, it can be utilized as auxiliary equipment for renewable energy, elimination of transmission congestion, frequency regulation service, voltage regulation service, peak reduction/shifting. In addition, it can be used as micro grid power/demand balance, frequency regulation, black start function in conjunction with micro grid, and it can be used as UPS (uninterruptible power system), peak reduction/shifting, DR (demand response) in behind-the-meter [1].

As mentioned above, various studies have been carried out because ESS can be utilized flexibly. When considering the economic return through ESS, it plays a different role depending on the participating market [2] and the role of ESS, which is a price-maker, as a price-maker to help lower the LMP (Locational Marginal Price) power price in the system, in response to the electricity price set by the price-taker [3], and a method for operating the LMP price so that the output uncertainty of the renewable energy is reduced [4].

In addition, various studies have been conducted depending on the ESS ownership and operation perspective. There are studies that the primary frequency response using the fast dynamic characteristics of BESS (battery energy storage system) [5], a study to assist the uncertain output of the wind turbine [6], the independent system operators (ISO) [7], a study on ESS as a part of MG and verification of linkage operation with MG (Micro Grid) internal operation and system [8].

In the case of KEPCO (Korea Electric Power Corporation), research focusing on frequency regulation rather than arbitrage and operation in the position of MG or the owner was performed. In the case of KEPCO, the institutional basis for the ESS to be used in the electric power market has not been established yet [9]. Therefore, research on frequency coordination services and renewable energy linkage is active from the point of view of system operation rather than part of operation of individual operators [5].

In this paper, we study the operation of grid scale ESS. Consideration was given to the operation of participating in the electric power market and profit taking, and the virtual SOC was considered in order to participate in different markets. Reference [10] also considered the reserve by considering the uncertainty. The difference between [10] and this study is that a certain amount of SOC is set as a specific value for reserve use in [10], but in this paper, it is advantageous that ESS has the advantage of operating in all modes of operation for high profits. Similar to this study, ESS was modelled to assess its impact on the Italian ancillary services market, taking into account the various operating modes of ESS [11]. Rossi's study [11] carried out detailed ESS modelling, but only considered operation for reserve purposes and did not distinguish SOC. In addition, [11] evaluated the impact and economic feasibility of ESS by considering the system through multi-year simulations. No detailed modeling was done as in [11]. However, we don't focus on detailed modeling and proposed a virtual SOC concept to participate in the energy market and auxiliary services market. In addition, in this study, the developed algorithm is tested by applying this to the demonstration system.

The main contributions in this study are as follows:

- Development of a day-ahead scheduling algorithm for grid-connected BESS in Korea Electricity market;
- Development of different power market participation methods using virtual SOC;
- Implementation and verification test of BESS demonstration system of developed algorithm using Matlab runtime.

The remainder of the paper consists of four sections. In Section 2, we discuss application of ESS in Korea power market. In Section 3, we describe engineering assumptions for the proposed algorithm model and the optimal scheduling algorithm modeling using MILP (Mixed Integer Linear Programming). The simulation results for the proposed algorithm performance are described in Section 4, and Section 5 describes the BESS demonstration system structure with the proposed algorithm, and conclusions and future research plans are presented in Section 6.

2. Application of Energy Storage System in Korea Power System or Market Participation

In Korea power market, the ESS is divided into three categories depending on the capacity, purposes: (1) central dispatch ESS, (2) non-central dispatch ESS, (3) ESS for transmission service operators. The central dispatch ESS is the ESS owned by a power generator that operates according to the power supply instructions of the KPX (Korea Power Exchange). In addition, the maximum discharge capacity exceeds 10 MW and the maximum operating time is more than 2 h. Or it is an ESS for frequency regulation service on a separate basis in KPX market rule. The non-central dispatch ESS is the ESS owned by a power generator not a central dispatch ESS. The ESS for transmission service operators is the ESS to provide system auxiliary services operated by the transmission operator. In this study, the non-central dispatch ESS is considered.

2.1. Arbitrage

In general, the arbitrage is a transaction that generates revenue by using price differences in two or more different markets. The electric energy arbitrage using the ESS is an economical operation that buys electricity at a cheap SMP (System Marginal Price) period and sells at an expensive SMP period through the ESS characteristic that can charge or discharge the electric energy.

In Korea power market, the charging/discharging energy through the non-central ESS is calculated by SMP. The SMP is defined each hour one day before. Therefore, the ESS owner which has a non-central dispatch ESS can operate to their economic benefit considering next day SMP. The ESS owner should make a charge/discharge profile using the characteristics of ESS. Especially, charging capacity and round trip efficiency have a significant impact. If the ESS rate capacity is the same, the round trip efficiency is high and the bigger the hourly SMP difference, the more economic benefit is expected.

2.2. Frequency Regulation

In Korea market, it is possible to participate in the frequency regulation (FR) service using the ESS. The FR service is divided into two categories: primary and secondary frequency responses. The primary frequency response is the frequency regulation capacity to initially respond to changes in system frequency and is the active power that can hold the power for more than 30 seconds within 10 seconds of changing the frequency. It generally means the governor free (G/F) of the generator and includes the frequency regulation function of the ESS. The secondary frequency regulation reserve is the active power for restoring to the normal frequency maintenance range after the primary FR. Additionally, it means that the AGC (Automatic Generation Control) of the generator can be sustained for 30 minutes by reacting within 30 seconds and EMS (Energy Management System) remote control of the ESS for the frequency regulation.

2.3. Renewable Energy Support

The domestic electric power market is introducing a new and renewable energy duty allocation system (RPS), and the power generation companies included in these targets are obliged to allocate a certain percentage of the supply amount as renewable energy. Renewable Energy Certificate (REC) means the unit by which the power of new and renewable energy is multiplied by the weight of the MWh-based power supplied from the facility to which the supply certificate is issued. In here, the meaning of 1 REC is the certification that 1 MWh is supplied with renewable energy.

At this time, the power generation company must fill in the mandatory quota by purchasing a certificate for the electric power produced from renewable energy, that is, REC from an individual company installing a new renewable power source directly or installing a new and renewable energy source.

In the case of this system, considering the domestic power market operating rules and the data notified by the Ministry of Industry, the ESS facility connected with the wind power facility applies the seasonal maximum load time criterion. The maximum load time for each season is the same as the following (Table 1).

Table 1. Seasonal maximum load time for energy storage system (ESS) installations.

Season	Date (mm.dd)	Peak Time (hour)
Spring	03.17–06.06	9–12
Summer	06.07–09.20	13–17
Fall	09.21–11.14	18–21
Winter	11.15–03.16	9–12

The weight of the ESS equipment is applied only to the amount of electric power discharged from the photovoltaic system in the time zone from 10 a.m. to 4 p.m. by discharging the battery at the other time zone in the case of the ESS equipment connected with the RPS target photovoltaic equipment. In the case of connected ESS equipment, applied every three years for ESS equipment connected with the RPS target wind power facility. This is applied only to the amount of electric power to be used by discharging (ESS → power system) during the seasonal maximum load time among charged electric power. The battery capacity standard meets the standards set by the director of the supply certification authority.

3. Scheduling Formulation

3.1. Description and Assumption

In order to perform various functions for possible driving methods through ESS, we have developed a function that maximizes economy by using optimization techniques and, consequently, generates commands for operating modes and output values by time zone as a result as shown in Figure 1. ESS is a facility that can contribute systemically through various functions such as energy difference transaction, new and renewable power assistance, and frequency regulation assistance service. The algorithm is designed to derive operation scheduling considering economic feasibility so that ESS can perform various functions on a daily basis.

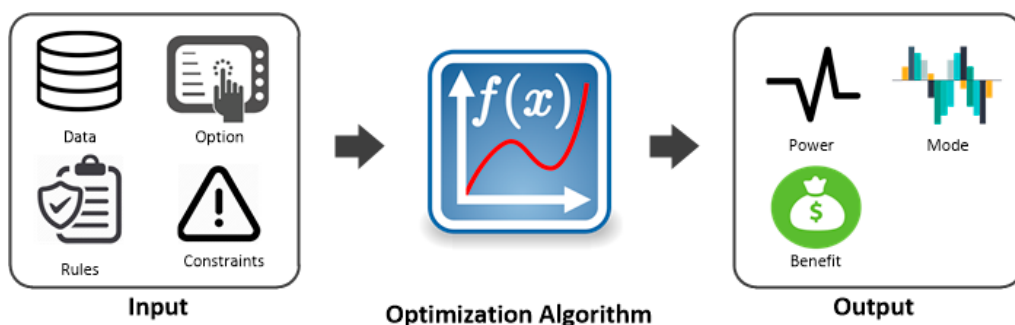


Figure 1. Optimization scheduling algorithm concept.

Several assumptions are made for the ESS optimization scheduling:

- The ESS can be operated by selecting an energy arbitrage, frequency regulation, and operation for REC weight for each time zone for their own benefit as a price taker.
- The ESS can select and operate different operating modes for different time zones.
- If the ESS is operating in FR at specific time, the SOC must be equal to the starting SOC of the time at the end of the operation mode.
- The ESS can divide SOC by SMP and SOC by wind energy and can make a profit separately.
- It is possible to operate both the arbitrage and the REC-weighted operation at the same time.

3.2. Objective Function

The day ahead scheduling algorithm draws the results of scheduling of ESS through an economic maximization objective function that considers three operation modes that take into account energy arbitrage, frequency regulation and REC-weighted operation. The objective function used the settlement unit price of each operating algorithm and the parameters in the current scheme, as shown in Equation (1).

$$\max f = \max \sum_{t=1}^{24} C_i(t) P_i(t) = \max \sum_{t=1}^{24} [C_1(t) P_1(t) + C_2(t) P_2(t) + C_3(t) P_3(t)]. \quad (1)$$

In Equation (1), P_i is the ESS output of i th mode and C_i is the price of the i th mode. In this system, the first mode is the energy arbitrage mode (ARBT) and $C_1(t)$ is hourly SMP. The second mode is the REC-weighted operation (REC) and $C_3(t)$ is the addition of the hourly SMP and REC value. The third mode is frequency regulation mode (FR) and $C_2(t)$ is the unit price for participating capacity of the frequency regulation service.

The ARBT mode expects revenue from SMP differences and the REC mode expects revenue from SMP differences and REC weights through discharge at specific times. The FR mode is defined as maintaining the specified SOC range during FR mode operation. The revenue in the FR mode is applied by multiplying the FR service unit price by participating capacity. When the ESS operates in FR, it has the SOC control that recovers to a certain SOC range. Therefore, it is considered that the ESS would be able to participate in the FR mode as each P_{rate} .

In this system, it considers one ESS SOC in three modes. Therefore, the system may be able to discharge the power charged in the ARBT mode to the REC mode. Therefore, SOC_1 and SOC_2 calculated by the power according to the operation modes are calculated in addition to the ESS SOC. Therefore, it is possible to buy and sell according to the each SOC according to the operation mode.

3.3. Constraints

Constraints are required in addition to the objective function as Equation (1) to perform the MILP. Constraints include ESS output limit, SOC calculation and operating range, and operating mode limitations. The constraints related to SOC are as follows.

$$SOC(t+1) = SOC(t) + [\eta_{ch} \frac{P_1^{ch}(t)}{E_{rate}} - \eta_{dch} \frac{P_1^{dch}(t)}{E_{rate}} + \eta_{ch} \frac{P_2^{ch}(t)}{E_{rate}} - \eta_{dch} \frac{P_2^{dch}(t)}{E_{rate}}] \times \Delta t, \quad (2)$$

$$SOC_1(t+1) = SOC_1(t) + [\eta_{ch} \frac{P_1^{ch}(t)}{E_{rate}} - \eta_{dch} \frac{P_1^{dch}(t)}{E_{rate}}], \quad (3)$$

$$SOC_2(t+1) = SOC_2(t) + [\eta_{ch} \frac{P_2^{ch}(t)}{E_{rate}} - \eta_{dch} \frac{P_2^{dch}(t)}{E_{rate}}], \quad (4)$$

$$10 \leq SOC(t) \leq 90, \quad (5)$$

$$SOC_{init} = SOC_{end} = 60, \quad (6)$$

$$SOC_1(0) = 20, SOC_2(0) = 30. \quad (7)$$

Equation (2) is the portion of the SOC calculation for the ESS. In addition, Equations (3) and (4) are the SOC calculation equation calculated by mode 1 and 2 of the ESS. Equation (5) is the constraints in the range of operation of SOC from 10% to 90%. Equation (6) is the constraint that equates the initial SOC to the final SOC and the value is applied to 60% in the simulation. Equation (7) is the initial value constraint for SOC_1 and SOC_2 . With the exception of at least 10% of SOC, the SOC_1 by ARBT mode is defined as 20% and SOC_2 by REC mode is defined as 30%. The parameter in Equations (5)–(7) can be changed by user definition.

$$0 \leq p_1^{dch}(t) \leq u_1^{dch}(t)P_{rate}, \quad (8)$$

$$0 \leq p_1^{ch}(t) \leq u_1^{ch}(t)P_{rate}, \quad (9)$$

$$0 \leq p_2^{dch}(t) \leq u_2^{dch}(t)P_{rate}, \quad (10)$$

$$0 \leq p_2^{ch}(t) \leq u_2^{ch}(t)P_{rate}, \quad (11)$$

$$0 \leq p_3^{dch}(t) \leq u_3^{dch}(t)P_{rate}, \quad (12)$$

$$0 \leq p_3^{ch}(t) \leq u_3^{ch}(t)P_{rate}, \quad (13)$$

$$0 \leq p_1^{dch}(t) \leq E_{rate} \times SOC_1(t), \quad (14)$$

$$0 \leq p_2^{dch}(t) \leq E_{rate} \times SOC_2(t). \quad (15)$$

Equations (8)–(15) are formulas for the output constraints of the ESS. The variables to be obtained from the developed MILP are constructed to calculate the charge output and the discharge output independently, and include the limit of the rated output having a positive value respectively. Therefore, it has output limit for two charge and discharge modes for each operation mode. Equations (14) and (15) are constraint condition expressions limited to discharge only when the dischargeable capacity for modes 1 and 2 is charged by the corresponding mode. Since only SOC_1 and SOC_2 are separately calculated according to the expressions Equations (2) and (3), only the capacity charged by the corresponding mode can be known, and it is possible to discharge only the capacity charged through the corresponding mode using the mode.

$$u_1^{dch}(t) + u_1^{ch}(t) \leq 1, \quad (16)$$

$$u_2^{dch}(t) + u_2^{ch}(t) \leq 1, \quad (17)$$

$$u_3^{dch}(t) + u_3^{ch}(t) \leq 1, \quad (18)$$

$$u_1^{dch}(t) + u_2^{ch}(t) \leq 1, \quad (19)$$

$$u_2^{dch}(t) + u_1^{ch}(t) \leq 1. \quad (20)$$

Equations (16)–(18) are constraints that charging or discharging can't be performed simultaneously for each operation mode. In addition, Equations (19) and (20) are constraint conditions that prevent ARBT and REC from having different output states.

$$0 \leq u_1^{dch}(t) \leq s_1(t), \quad (21)$$

$$0 \leq u_1^{ch}(t) \leq s_1(t), \quad (22)$$

$$0 \leq u_2^{dch}(t) \leq s_2(t), \quad (23)$$

$$0 \leq u_2^{ch}(t) \leq s_2(t), \quad (24)$$

$$0 \leq u_3^{dch}(t) \leq s_3(t), \quad (25)$$

$$0 \leq u_3^{ch}(t) \leq s_3(t). \quad (26)$$

Equations (21)–(26) are binary constraints for the operation mode, and is expressed as 0 when the operation mode is not operated, so that the charge/discharge state variable cannot be selected and cannot have a value of 1. If a specific operation mode is activated, it is possible to select the state of charge and discharge in this case.

$$s_1(t) + s_2(t) \leq 1, \quad (27)$$

$$s_1(t) + s_2(t) + s_3(t) \leq 1, \quad (28)$$

$$s_1(t) + s_3(t) \leq 1, \quad (29)$$

$$s_2(t) + s_3(t) \leq 1. \quad (30)$$

Equations (27)–(30) are constraints on the operation mode that can operate simultaneously for operation mode 1 and 2. In this system, ARBT and REC are supposed to be able to operate at the same time, so that the mode constraint is limited to 2 or less as in Equations (27) and (28). In Equation (28), if the right term is defined as 2, two operation modes can be operated at the same time. Equations (29) and (30) are constraints that mean that the ARBT and REC modes cannot operate at the same time as

the FR mode. If the right side of the constraints (27) and (28) is changed to 1, only one operation mode is executed. The effect of these changes is simulated and analyzed in Section 4.

$$s_3(t) \leq -SOC(t) + 1 + FR_{ubsoc}, \quad (31)$$

$$s_3(t) \leq \frac{SOC(t)}{FR_{lbsoc}}, \quad (32)$$

$$FR_{ubsoc} = \begin{cases} 0.8 & C - rate \leq 1 \\ 0.75 & 1 \leq C - rate \leq 4, \\ 0.7 & 4 \leq C - rate \end{cases} \quad (33)$$

$$FR_{lbsoc} = \begin{cases} 0.5 & C - rate \leq 1 \\ 0.55 & 1 \leq C - rate \leq 4. \\ 0.6 & 4 \leq C - rate \end{cases} \quad (34)$$

Equations (31) and (32) are constraint conditions for setting the operation range in which the frequency regulation service, which is the third operation mode, can operate. In this system, it is assumed that the SOC does not fluctuate according to the output when the frequency regulation service is engaged, and is equal to the SOC of the start time at the end of the operation time of the operation mode. However, due to the nature of the frequency tuning operation, it is considered that operation is not possible at low SOC or high SOC. Therefore, it is necessary to maintain the SOC within the applicable operating range by setting the operating range (FR_{ubsoc} , FR_{lbsoc}) respectively. For example, if $FR_{ubsoc} = 0.7$, $FR_{lbsoc} = 0.5$, Equation (31) cannot be turned on because SOC is 0.7 or higher and the right-hand side has a value of 1 or less. Equation (32) is also a constraint that if the SOC is not greater than 0.5, the right term cannot be turned on if it is less than 1.

Equations (33) and (34) are the operating ranges of the FR SOC according to the C-rate.

In the case of frequency regulation, there is no SOC constraint as shown in Equation (2) above. This is because it is assumed that there is no loss of energy when the SOC is terminated when participating through the SOC recovery control in the case of frequency regulation. However, we concluded that it is not reasonable to have the same SOC operating range in ESS with lower capacity than output. In case of outputting by participating in the frequency regulation with the same capacity, since the fluctuation of the ESS SOC having a high C-rate is large, the operation ranges in which the frequency regulation can be performed is reduced as the C-rate is increased. The higher the C-rate, the smaller the operating range, and the operating range was calculated to be more than 50% since the discharge is usually performed during frequency control. The C-rate means the performance of the ESS power with respect to its rated capacity.

$$0 \leq P_{wind}(t) \times Wind_{margin} - p_2^{ch}(t). \quad (35)$$

Equation (35) is a constraint on the limitation of wind power generation. It is a formula that limits the expected amount of wind power generation by the time of day to not allow any further charging in consideration of the margin. This is a constraint on the actual chargeable power (P_2).

4. Case Study

4.1. Description

The proposed day-ahead scheduling algorithm was simulated based on real data and had a time step of 1-hour period. The predicted value of wind power generation was modified by applying the seasonal seawater wind power value. The simulation simulated ESS with each 1,2,4 C-rate in three SWPLCs (Soft Programmable Logic Controllers). This is a scheduling algorithm applied to the BESS demonstration system and is described in detail in the following section. The main parameters of the

ESS applied to the simulation are shown in Table 2 below. Considering the system such as battery, PCS, etc., charging/discharging efficiency was assumed to be 90% and P_{ratio} was 70%. These two parameters were planned to be applied to SWPLC efficiency and optimal P_{ratio} value by analyzing the results of the verification test. The start and end set values of the SOC are also planned to be supplemented by analyzing the result of the verification test in the future to apply the optimum value.

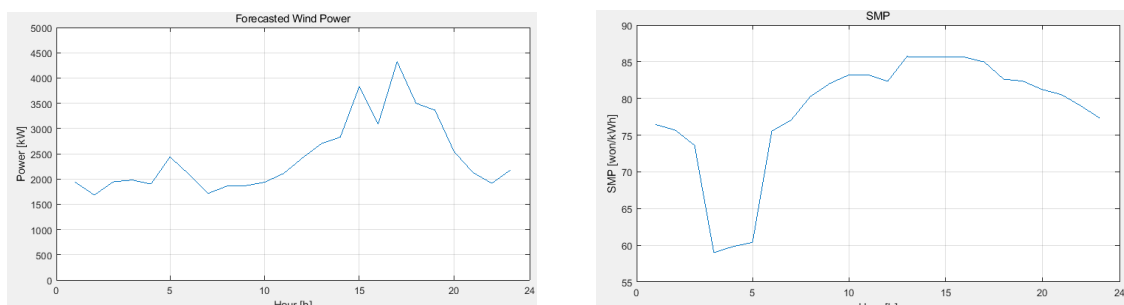
Table 2. Simulation parameters and applied values.

Variable	Parameter	Unit	Description
P_{rate}	4000 4000	kW	ESS Rated Power
E_{rate}	2000 1000	kWh	ESS Rated Capacity
ESS_{eff}	90	%	ESS charging/discharging efficiency
SOC_{init}	60	%	Initial SOC
SOC_{end}	60	%	Final SOC
SOC_{lo}	10	%	SOC Lower Limit
SOC_{up}	90	%	SOC Upper Limit
SOC_{1_init}	20	%	SOC for Arbitrage mode Initial SOC
SOC_{2_init}	30	%	SOC for REC mode Initial SOC
SOC_{1_end}	20	%	SOC for Arbitrage mode Final SOC
SOC_{2_end}	30	%	SOC for REC mode Final SOC
P_{ratio}	70	%	ESS Power Limit
FR_{price}	3.24	Won/kW	Frequency Regulation Unit Price
REC_{price}	95,000	Won/REC	REC Unit Price
REC_{weight}	5	-	REC Weight

4.2. Simulation Results

In order to verify the performance of the day-ahead scheduling algorithm, various cases were simulated and analyzed. We applied summer data for the base scenario and simulated the operation mode concurrency and final SOC constraint for comparative analysis.

Figure 2 shows common SMP data and wind power forecast data. Grid-connected ESS, in conjunction with wind power generators, gives priority to the economics of ESS providers. In the present system, the simulation time step is one hour because the charge is settled in 1-hour. In addition, even when the REC weighting is in operation, the discharge amount is set to the amount of time. The predicted value of the wind power generation was applied based on the average wind speed per hour, and it was assumed that the actual system operation was controlled so that the real time measurement value was not exceeded the value multiplied by $Wind_{margin}$. Additionally, in the FR operation mode, the FR was measured by measuring the frequency in real time, and it was assumed that the SOC was recovered at the end of the FR operation mode as previously assumed.



(a) Forecasted Wind Power

(b) SMP

Figure 2. Simulation common input data.

4.2.1. Scenario 1

In Scenario 1, only one operation mode per time zone was operated and initial $SOC_1 = 20\%$ and $SOC_2 = 30\%$ were simulated. SOC_1 and SOC_2 were also limited to the same initial values at the end of the simulation.

Figure 3 shows the simulation results of Scenario 1. This figure shows the power, SOC, and operation mode for each SWPLC. In the output graph, the blue bar means output by ARBT and the red bar means output by REC. In the graph of the time mode operation mode, the blue bar indicates the ARBT, the red bar indicates REC, the yellow bar indicates FR, and the purple bar indicates an idle state. In the output graph, the frequency regulation service participation capacity is not expressed as output, because it is assumed that it can participate at the maximum capacity. Comparing Figure 3 (a), (d), (g), it can be seen that no discharge occurs at dawn at SWPLC #3 with high C-rate. This means that the REC weighting time in summer is 1–3 p.m. and that REC * w can be expected in SMP. Therefore, it is necessary to charge the SOC_2 so that it discharges as much as the SOC_1 that was charged with the initial ARBT and discharges to the REC. Therefore, it can be confirmed that the large capacity SWPLC 1 and 2 are discharged before 4 or 5 a.m. when the SMP is low, and charged to P_2 by the maximum SOC for participating in the frequency regulation. After that, it can be confirmed that SOC is discharged up to 90% immediately before 1 p.m. and to SOC 10% between 1 p.m. and 3 p.m. after charging. In contrast, the third SWPLC with a low capacity has a small SOC range for participating in the frequency regulation service, and the amount of charge required to discharge the maximum is smaller than the rated value of the wind turbine generator. After 11–12 a.m., it discharges to P_1 and charges between P_2 and 12–13 a.m. to secure capacity. After the REC weighting time period, it is confirmed that the ARBT charges the SOC_1 constraint 20% REC constraint SOC 30% as in the case of the initial constraint.

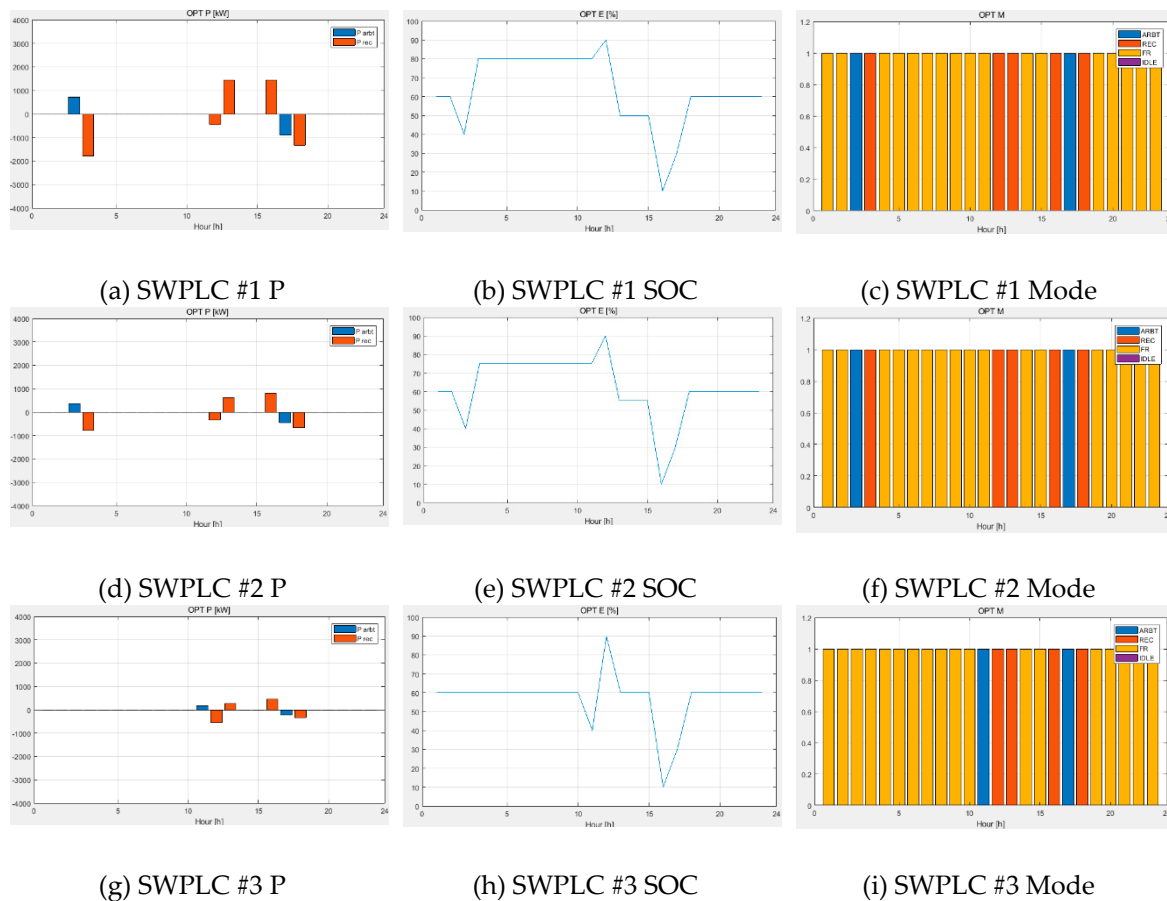


Figure 3. Scenario 1 simulation results.

4.2.2. Scenario 2

Scenario 2 is the same as Scenario 1, except that only the final SOC_1 and SOC_2 constraints are excluded. The effect of the final SOC_1 and SOC_2 constraints on scheduling can be confirmed through Scenario 2.

Figure 4 shows the simulation results of Scenario 2. Compared with Figure 3, it can be seen that until the time of 1 p.m. to receive the REC weight, the two pictures have the same pattern. As shown in Figure 3, when ARBT and REC are operated for 1 hour after 5 p.m., it can be confirmed that SOC is restored by only charging by ARBT. This is because, unlike Scenario 1, the final value is not limited to SOC_1 and SOC_2 , it is only recovered to SOC_1 charged by SMP. In the simulation, the ARBT is applied to the KPX market which is settled by the SMP and is settled as the REC value is added to the normal SMP even if the weighting is not applied for the REC weight operation. Therefore, the ESS can be confirmed that the ARBT mode is charged to a lower value than the REC mode. In other words, ARBT is calculated by SMP and REC by SMP+REC.

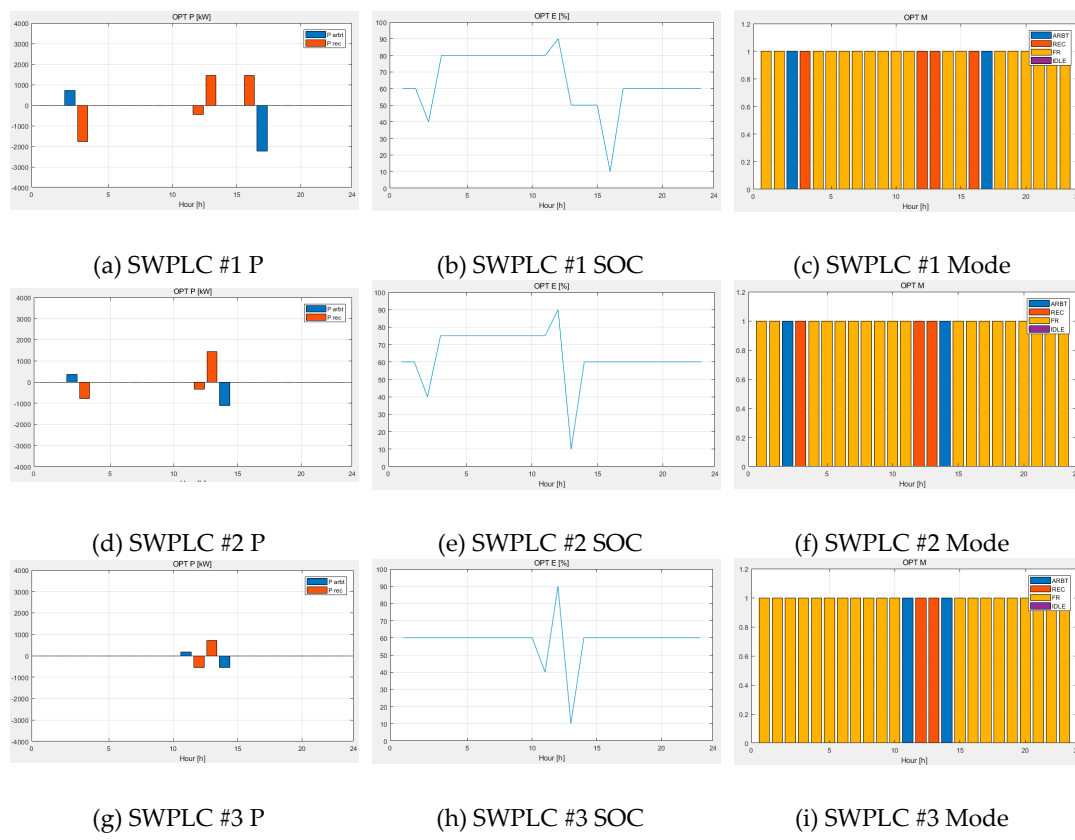


Figure 4. Scenario 2 simulation results.

4.2.3. Scenario 3

Scenario 3 simulated a 15% lower forecast of wind power than before. Figure 5 shows wind power forecast data used in Scenario 3.

Figure 6 is the simulation result of Scenario 3. Figure 6 shows that the output and output mode graphs for each SWPLC show more charging instructions in REC mode than in previous scenarios. Earlier, it was assumed that three wind turbines were rated at 3 MW and were associated with one SWPLC. Thus, in the previous scenario, the forecast wind power of about 2 MW/hour could be charged for an hour with enough capacity, compared to the forecast wind power of about 1 hour, requires a lot of time for sufficient capacity. Therefore, many REC output modes are required at 1 C-rate SWPLC with a higher rated capacity, and many REC output modes are not required because the

higher the C-rate. C-rate is generally the ratio of the output to the rated capacity of the ESS. Figure 7 shows an output graph of wind power generation by SWPLC combined with ESS. As shown in Figures 6a and 7a, the SWPLC at the 1 C-rate has a lot of capacity required for revenue from expensive REC operations, indicating that the charge is high at dawn. In Figure 7a, considering $Wind_{margin}$, it can be seen that almost all wind power is charged from ESS. By comparison, in Figure 7b,c, you can see that the charge is less time than SWPCL #1. However, SWPLC #2, #3 can be found to be involved in frequency regulation after charging for a small amount of time due to low demand capacity. Thus, if the rated capacity of wind farms versus ESS is higher, the ESS with high C-rate is expected to operate similar to other days when low wind speeds are expected, while the ESS with low C-rate is likely to charge wind power for a long time. After discharge for REC weights after 12 p.m., the charging schedule is set for the constraints SOC_1 , SOC_2 . Additionally, as with earlier charging, the 1C-rate SWPLC can be seen to require a lot of time to discharge.

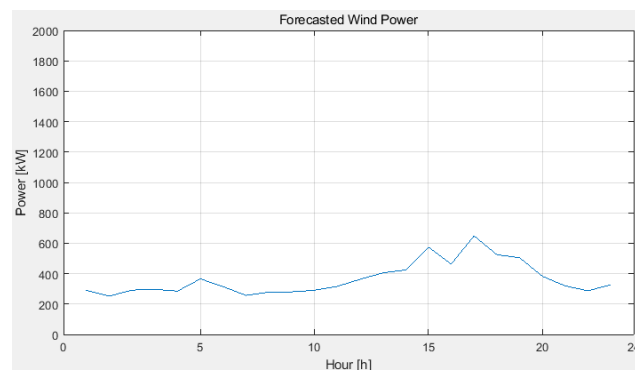


Figure 5. Scenario 3 wind power.

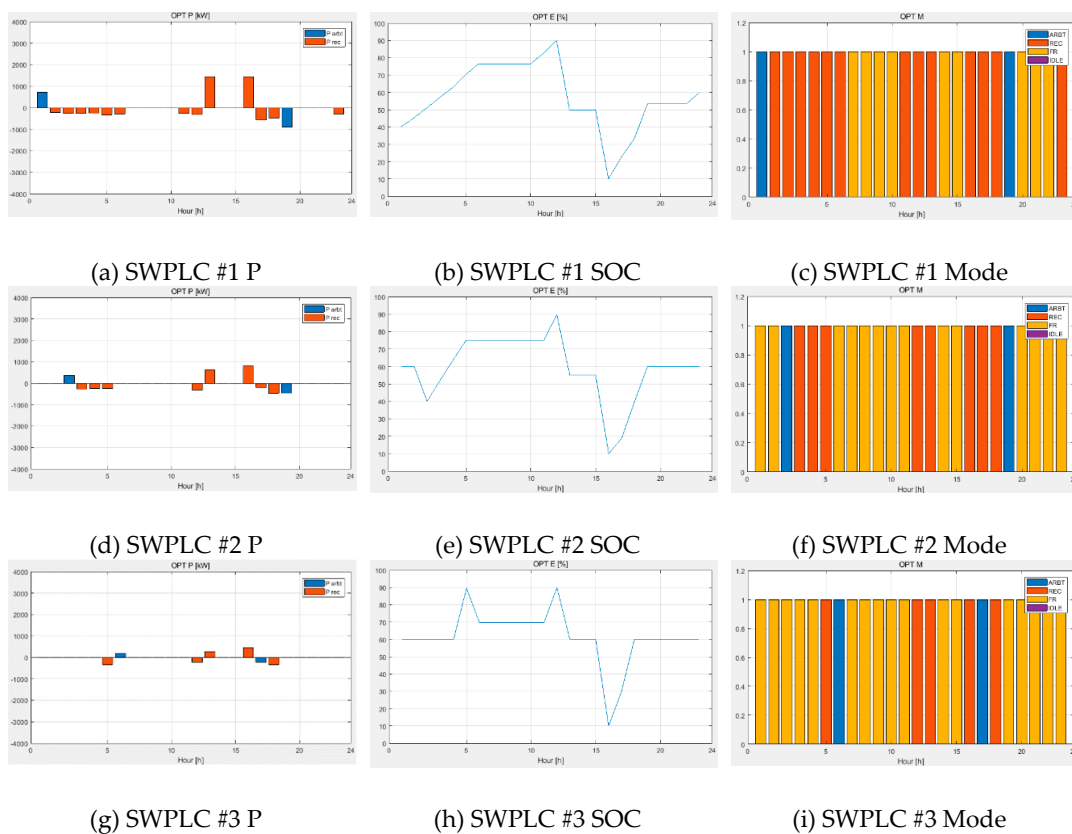


Figure 6. Scenario 3 simulation results.

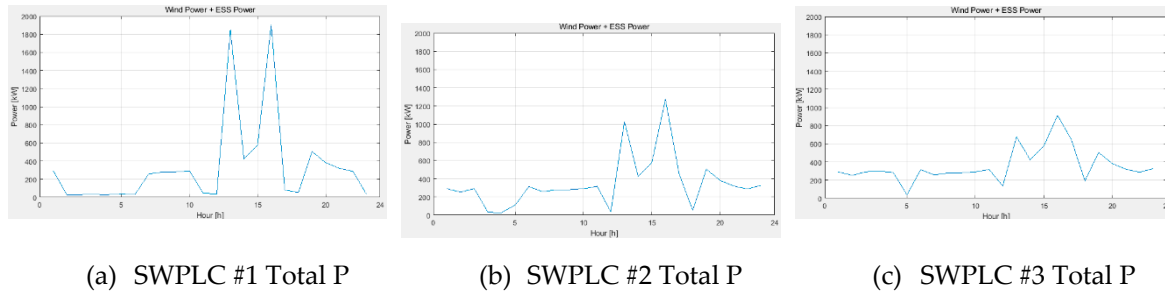


Figure 7. Hourly wind and energy storage system (ESS) power (in Scenario 3).

4.2.4. Scenario 4

Scenario 4 simulated the CPP (Critical Peak Price) situation. Although there is no CPP in the Korean electric power market, it is assumed that CPP is introduced. This is the same as the input data of Scenario 1 except that the SMP of 6–7 p.m. is increased five times.

Figure 8 shows the input data for Scenario 4. As can be seen in Figure 8, the SMP of 6–7 p.m. is higher, and thus the REC price is also higher. However, even if a CPP occurs, it does not reach the REC price of the REC weighting time 1–3 p.m. Figure 8 shows the simulation results of Scenario 4, and only the results of 1 C-rate and 4 C-rate SWPLC are shown in order to confirm the difference according to the characteristics by C-rate. As a result, SWPLC # 1 with a high C-rate shows a pattern that does not discharge SOC_1 at dawn time, unlike before. Therefore, it can be confirmed that SOC is recovered by charging SOC_1 immediately after discharge only by excluding SOC_2 . from SOC 90% at 1–2 p.m. It can be confirmed that the FR participates in the FR for two hours before 6–7 p.m. when the CPP occurs, and then it is confirmed that the CPP is discharged at the time of occurrence. Figure 9d,f shows the SWPLC simulation result of the 4 C-rate. Unlike the simulation result of the 1 C-rate, it can be confirmed that charging and discharging are performed using the minimum time because the capacity is low compared to the rated output. In the case of SWPLC # 1, the discharge is performed at 1–2 p.m., which gives the REC weight, and the SOC is maintained at 60% due to the charging by P_1 . On the other hand, in SWPLC # 3, the rest is discharged at 4–5 p.m., the SOC_1 is charged at 5–6 p.m. P_1 , and the CPP is discharged at 6–7 p.m. Therefore, it can be confirmed that the discharge is maximally discharged by the capacity of the discharge by the REC, and the charge is discharged after the maximum charge even when the CPP occurs.

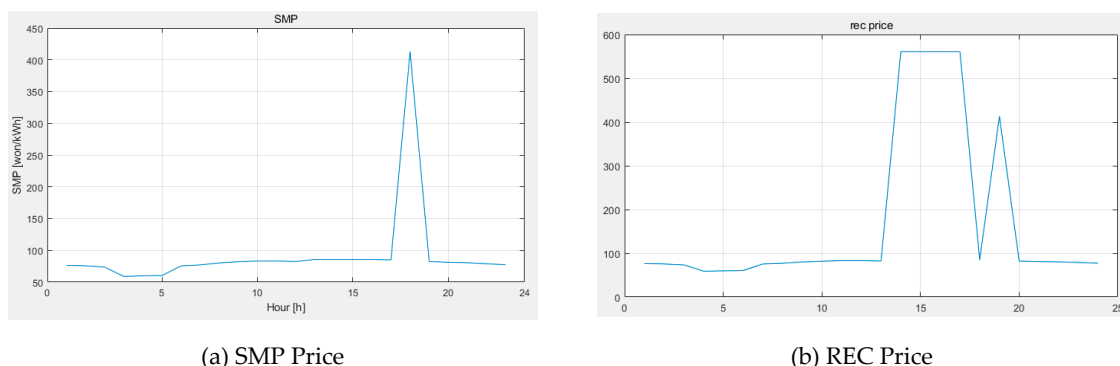


Figure 8. Input data with Critical Peak Price (CPP) (in Scenario 4).

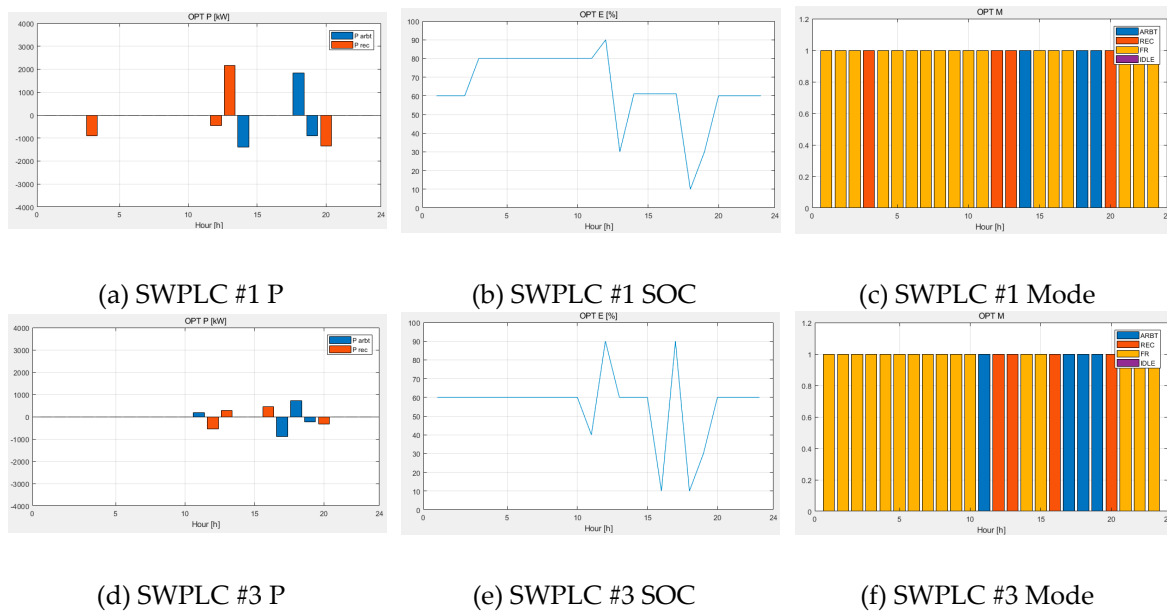


Figure 9. Scenario 4 simulation results.

4.2.5. Scenario 5

Scenario 5 is a scenario in which it is assumed that two operation modes can be operated simultaneously. Equations (27) and (28) are defined as two with the same input data as Scenario 1. Equation (27) is a constraint on whether ARBT and REC modes can be operated at the same time. It is assumed that SOC can be calculated by virtual SOC because two operation modes participate in the market that performs settlement for the participating capacity. Equations (29) and (30) do not change because the frequency tuning service cannot operate simultaneously with the ARBT or REC operating modes.

Figure 10 shows the simulation results of Scenario 5. In contrast to the results of Scenario 1, Figure 10a shows that there are two outputs at the same time for one hour to recover the final SOC. In Figure 10 (c), two additional clocks are active at the same time, but the actual output is 0 and only the discharge P_2 by REC is active. Other than that, the simulation result of Scenario 1 is the same as the result of simulation of SWCLC # 1, except for the part for the final SOC recovery.

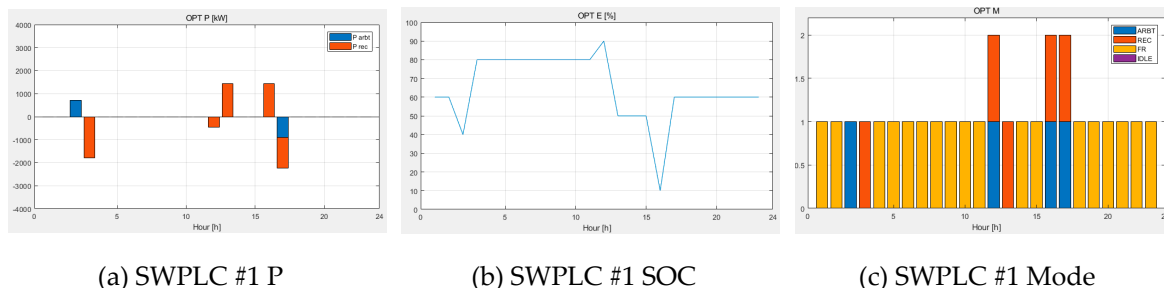


Figure 10. Scenario 5 simulation results.

4.2.6. Results

Table 3 shows the expected returns based on the ESS schedule for each scenario. It can be seen that Scenario 2, which has no limit on the final SOC, compared with Scenario 1, has a higher loss due to charging due to charging at the time of charging to meet the restriction, and thus the expected profit of Scenario 2 is higher. Scenario 3 is a scenario using forecasted wind power generation amounting to only 15% of that of Scenario 1, and SWPLC # 1 is used to charge SOC two more times than Scenario

1. Therefore, SWCC # 3 with high C-rate is not significantly affected by the high capacity of wind turbine connected to ESS capacity. We can see that the profit is similar. Scenario 4 simulated the occurrence of CPP, and because of the opportunity to discharge expensively, the revenue of SWPLC # 3, which discharged as much as possible in both REC weighting time and CPP, increased by about 36%. In Scenario 5, it is assumed that two operation modes can be operated simultaneously for one hour, and it can be confirmed that profit is slightly increased as compared with the Scenario 1. This is expected profit because it is possible to participate in frequency regulation service for one hour because the difference of charge of SOC_1 and SOC_2 does not change during final SOC recovery compared with existing scheduling but can be done for one hour.

Table 3. Simulation parameter and applied value.

Scenario	SWPLC Number	Benefit [Won]
1	1	1,496,641
	2	855,877
	3	543,705
2	1	1,633,148
	2	942,960
	3	600,211
3	1	1,380,803
	2	814,633
	3	536,588
4	1	1,754,622
	3	740,776
5	1	1,506,481

5. ESS Demonstration System

The algorithms proposed in the previous section were applied to the BESS demonstration test center. The BESS demonstration system was constructed at the Korea Electric Power Corporation Testing Center in Gochang, Korea as shown in Figure 11. The BESS has a total of 28 MW/17 MWh and consists of one TEMS (Total Energy management System) that monitors and controls the entire BESS system, three LPMS (Local Power Management System) that monitors and controls each of 1,2,4 C-rates, and seven SWPLCs that monitor and control the ESS under the LPMS. It is constructed as shown in Figure 12. The scheduling algorithm applied is performed in units of SWPLC in the LPMS. LPMS is applied to algorithms by receiving data from TEMS such as market information. The reason for the differences in the number of connections between SWPLC and the PCS is that the various PCS manufacturers are comprised of various PCS manufacturers, taking into account the communication methods and units of each PCS manufacturer.



Figure 11. KEPCO Gochang BESS demonstration system.

As noted in the previous paragraph, the algorithms proposed in this study were applied to the LPMS. The data required to perform this algorithm (SMP, Wind Forced P) is stored in the DB after 6

p.m. the day before the target date and the optimization schedule is performed at 11 p.m. In the LPMS, each SWPLC is scheduled and stored in the DB. The SWPLC receives the scheduling result from the DB and operates it according to the output mode and the operation mode according to the time zone.

The BESS monitoring control program at TEMS is made with C++. This algorithm simulated with Matlab is linked to the TEMS program by utilizing Matlab Runtime. The TEMS program consisted of a function to perform the optimization algorithm on a cycle basis. Within the function, the scheduling algorithm is performed by reading the data required for optimized scheduling from the DB. Using Matlab runtime, functions provided by Matlab can also be used for C++. In this system, Matlab Runtime was performed by setting the MILP model in Matlab as input/output data according to the purpose function. The performance results are derived as a result of the array types of output, SOC, and operational modes, and the algorithm is terminated by storing them in the DB.

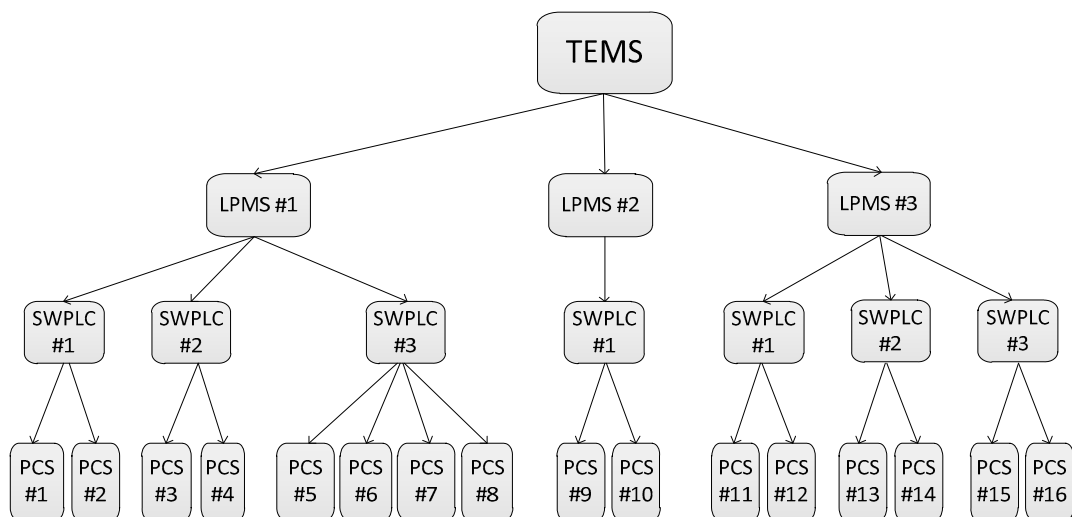


Figure 12. ESS demonstration structure.

Figure 13 is the result of Matlab simulation for a specific scenario in LPMS in 1C-rate BESS, and Figure 14 is the HMI in TEMS in the same scenario. Figure 13 previously simulated no final SOC_1 , SOC_2 , with the initial $SOC_1 = 0\%$ and $SOC_2 = 50\%$ in Scenario 1 of the Section 4.1. Therefore, since there is no SOC_1 compared to Scenario 1 in Chapter 4, it can be seen that there is a pattern of maxing out SOC_2 in order to discharge it to the expected REC. Since there are no additional constraints after discharging at the time when the REC weight is assigned at 1–3 p.m., it is possible to verify that the SMP is charged to the SOC constraint and then participates in the FR. This can be seen as the same in Figure 14. Figure 14 shows the result of scheduling by SWPLC in the demonstration system. The figure shows the scheduling result interface of the LPMS with three SWPLCs. In the figure, blue is the ARBT mode, red is the G/F mode, green is the REC mode, and the actual output and p.u. values of the output are expressed together. In addition, at the top of the schedule, the expected revenue for each SWPLC is presented together. The software of the BESS demonstration system is constructed as shown in Figure 12. Figure 13 is planned to conduct operational functions and control tests of the various BESSs with the associated offshore wind generator and dummy load in the future.

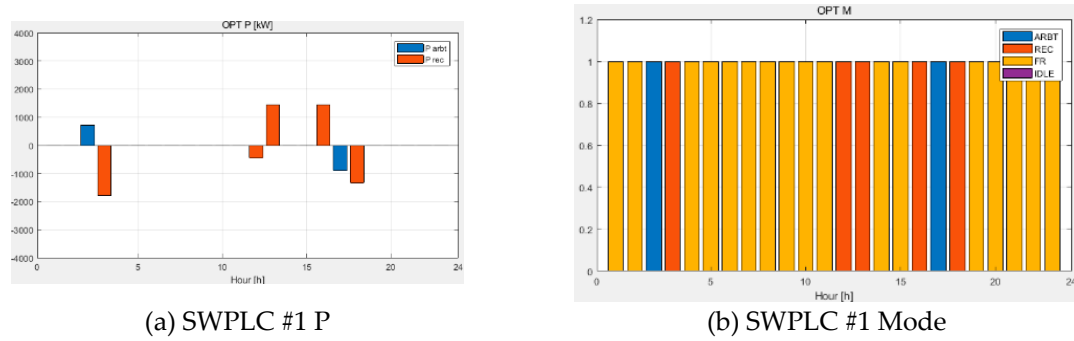


Figure 13. Scheduling results in TEMS.



Figure 14. Scheduling results in TEMS.

6. Conclusions and Future Works

It has been installed and operated for many purposes due to the characteristics of ESS and the drop in installation cost due to technological development. In this paper, we have developed a scheduling algorithm to maximize the profit of the ESS owner for the operation modes that can be participated by using ESS in KEPCO market, SMP and the frequency regulation service for receiving the REC weight of the connected renewable energy source. The objective function of the optimal scheduling is modeled to maximize the profit settled by each participating capacity. However, since the KEPCO market does not guarantee the participation of free ESS in the market, it assumes some situations. Typically, frequency regulation service is not suitable for full-day scheduling and differs from energy actually used. It is assumed that we have a recovery control algorithm that can maintain the SOC of time. In addition, the characteristics of the ESS are considered by defining the SOC range of the ESS participating in the frequency regulation service differently for each C-rate. The developed optimal scheduling objective function is solved by MILP and performance verification is performed through various scenarios in Matlab environment. The results of the simulation show that the C-rate has a different schedule even under the same conditions. This is because it operates in the favorable operation mode considering the characteristics of each ESS according to the difference between the capacity involved in the frequency regulation service and the output capacity. At this time, SMP is similar by season and by day, so it can be expected that similar expected profit will be generated for a long time. Therefore, it is also possible to estimate the appropriate capacity of the wind turbine connected to each ESS by analogy with the result of simulating the difference of wind power generation.

In addition, the developed scheduling algorithm has been installed in the demonstration system of KOPCO's Gochang BESS test center. We developed the algorithm to derive the scheduling results for each SWPLC and to execute the algorithm using the Matlab runtime function with the operating program. It can be confirmed that the same scheduling result as that of the simulation result is derived and operated even through the constructed demonstration system.

Future studies will be carried out in the demonstration system for performance verification and testing of various conditions. Since the developed algorithm is a day-ahead scheduling, it will be supplemented to perform real-time scheduling in consideration of uncertainty of renewable energy. In the study, charge/discharge efficiency and P_{ratio} were set to fixed values. However, the empirical operating data will be analyzed to derive the P_{ratio} value for the actual charge/discharge efficiency and optimal efficiency. Additionally, the development algorithm will be used to raise the issue of participation of ESS in the electric power market in Korea Electric Power Market and the research will be supported to support the policy proposal.

Author Contributions: H.-J.C. prepared the manuscript and completed the simulations. S.-E.L. discussed the results and D.W. commented on the manuscript. All of the authors read and approved the final manuscript.

Acknowledgments: This work was supported by the Power Generation & Electricity Delivery Core Technology Program of the Korea Institute of Energy Technology Evaluation and Planning (KETEP), granted financial resource from the Ministry of Trade, Industry & Energy, Republic of Korea. (No.20142010103010) This research was supported by Korea Electric Power Corporation. (Grant number: R18XA01)

Conflicts of Interest: The authors declare no conflict of interest.

References

1. Salles, M.B.C.; Aziz, M.J.; Hogan, W.W. Potential arbitrage revenue of energy storage systems in PJM during 2014. In Proceedings of the 2016 IEEE Power and Energy Society General Meeting (PESGM), Boston, MA, USA, 17–21 July 2016; pp. 1–5.
2. Suazo-Martínez, C.; Pereira-Bonvallet, E.; Palma-Behnke, R.; Zhang, X. Impacts of Energy Storage on Short Term Operation Planning Under Centralized Spot Markets. *IEEE Trans. Smart Grid* **2014**, *5*, 1110–1118. [[CrossRef](#)]
3. Mohsenian-Rad, H. Coordinated Price-Maker Operation of Large Energy Storage Units in Nodal Energy Markets. *IEEE Trans. Power Syst.* **2016**, *31*, 786–797. [[CrossRef](#)]
4. Degeilh, Y.; Gross, G. Stochastic Simulation of Utility-Scale Storage Resources in Power Systems with Integrated Renewable Resources. *IEEE Trans. Power Syst.* **2015**, *30*, 1424–1434. [[CrossRef](#)]
5. Cho, S.-M.; Yun, S.-Y. Optimal Power Assignment of Energy Storage Systems to Improve the Energy Storage Efficiency for Frequency Regulation. *Energies* **2017**, *10*, 2092. [[CrossRef](#)]
6. Halamay, D.; Antonishen, M.; Lajoie, K.; Bostrom, A.; Brekken, T.K.A. Improving Wind Farm Dispatchability Using Model Predictive Control for Optimal Operation of Grid-Scale Energy Storage. *Energies* **2014**, *7*, 5847–5862. [[CrossRef](#)]
7. Khani, H.; Zadeh, M.R.D.; Varma, R.K. Optimal scheduling of independently operated, locally controlled energy storage systems as dispatchable assets in a competitive electricity market. *IET Gener. Transm. Distrib.* **2017**, *11*, 1360–1369. [[CrossRef](#)]
8. Choi, S.; Min, S. Optimal scheduling and operation of the ESS for prosumer market environment in grid-connected industrial complex. In Proceedings of the 2017 IEEE Industry Applications Society Annual Meeting, Cincinnati, OH, USA, 1–5 October 2017; pp. 1–7.
9. Hur, W.; Moon, Y.; Shin, K.; Kim, W.; Nam, S.; Park, K. Economic Value of Li-ion Energy Storage System in Frequency Regulation Application from Utility Firm’s Perspective in Korea. *Energies* **2015**, *8*, 5000–5017. [[CrossRef](#)]
10. Gantz, J.M.; Amin, S.M.; Giacomoni, A.M. Optimal Capacity Partitioning of Multi-Use Customer-Premise Energy Storage Systems. *IEEE Trans. Smart Grid* **2014**, *5*, 1292–1299. [[CrossRef](#)]
11. Rossi, A.; Stabile, M.; Puglisi, C.; Falabretti, D.; Merlo, M. Evaluation of the energy storage systems impact on the Italian ancillary market. *Sustain. Energy Grids Netw.* **2019**, *17*, 100178. [[CrossRef](#)]



© 2019 by the authors. Licensee MDPI, Basel, Switzerland. This article is an open access article distributed under the terms and conditions of the Creative Commons Attribution (CC BY) license (<http://creativecommons.org/licenses/by/4.0/>).